



The Class II Trehalose 6-phosphate Synthase Gene *PvTPS9* Modulates Trehalose Metabolism in *Phaseolus vulgaris* Nodules

OPEN ACCESS

Edited by:

Wim Van den Ende,
KU Leuven, Belgium

Reviewed by:

Astrid Wingler,
University College Cork, Ireland
Christian Meyer,
French National Institute for
Agricultural Research (INRA), France

***Correspondence:**

Claudia Díaz-Camino
claudia@ibt.unam.mx
Carmen Quinto
quinto@ibt.unam.mx

† Present Address:

Aarón Barraza,
CONACYT. Centro de Investigaciones
Biológicas del Noroeste S. C. Instituto
Politécnico Nacional No. 195. La Paz,
Mexico;
Cecilia Contreras-Cubas,
Instituto Nacional de Medicina
Genómica, Arenal Tepepan, Mexico

‡ In loving memory.

Specialty section:

This article was submitted to
Plant Physiology,
a section of the journal
Frontiers in Plant Science

Received: 24 August 2016

Accepted: 07 October 2016

Published: 01 November 2016

Citation:

Barraza A, Contreras-Cubas C,
Estrada-Navarrete G, Reyes JL,
Juárez-Verdayes MA, Avonce N,
Quinto C, Díaz-Camino C and
Sanchez F (2016) The Class II
Trehalose 6-phosphate Synthase
Gene *PvTPS9* Modulates Trehalose
Metabolism in *Phaseolus vulgaris*
Nodules. *Front. Plant Sci.* 7:1589.
doi: 10.3389/fpls.2016.01589

Aarón Barraza^{1†}, Cecilia Contreras-Cubas^{1†}, Georgina Estrada-Navarrete¹,
José L. Reyes¹, Marco A. Juárez-Verdayes¹, Nelson Avonce², Carmen Quinto^{1*},
Claudia Díaz-Camino^{1*} and Federico Sanchez^{1‡}

¹ Departamento de Biología Molecular de Plantas, Instituto de Biotecnología/Universidad Nacional Autónoma de México, Cuernavaca, Mexico, ² Centro de Investigación en Dinámica Celular, Universidad Autónoma del Estado de Morelos, Cuernavaca, Mexico

Legumes form symbioses with rhizobia, producing nitrogen-fixing nodules on the roots of the plant host. The network of plant signaling pathways affecting carbon metabolism may determine the final number of nodules. The trehalose biosynthetic pathway regulates carbon metabolism and plays a fundamental role in plant growth and development, as well as in plant-microbe interactions. The expression of genes for trehalose synthesis during nodule development suggests that this metabolite may play a role in legume-rhizobia symbiosis. In this work, *PvTPS9*, which encodes a Class II trehalose-6-phosphate synthase (TPS) of common bean (*Phaseolus vulgaris*), was silenced by RNA interference in transgenic nodules. The silencing of *PvTPS9* in root nodules resulted in a reduction of 85% ($\pm 1\%$) of its transcript, which correlated with a 30% decrease in trehalose contents of transgenic nodules and in untransformed leaves. Composite transgenic plants with *PvTPS9* silenced in the roots showed no changes in nodule number and nitrogen fixation, but a severe reduction in plant biomass and altered transcript profiles of all Class II TPS genes. Our data suggest that *PvTPS9* plays a key role in modulating trehalose metabolism in the symbiotic nodule and, therefore, in the whole plant.

Keywords: Class II trehalose-6-phosphate synthase, trehalose biosynthetic pathway, legume-rhizobium symbiosis signaling, AGO1-complex, *Phaseolus vulgaris* (common bean)

INTRODUCTION

Legumes have symbiotic relationships with rhizobial soil bacteria, which results in the formation of nitrogen-fixing nodules on the roots of the plant host. Thanks to this remarkable association, leguminous plants can grow in nitrogen-poor environments. However, the biological fixation of nitrogen is energetically expensive; to support growth, plants must maintain a delicate balance that ensures sufficient fixed nitrogen without depleting their carbon reserves. One way in which legumes achieve this balance is by regulating the final number of nodules in the root (Gage, 2004; Ferguson et al., 2010; Kouchi et al., 2010).

Molecular genetic analyses in model legume species have shown that legumes inhibit nodulation by systemic signals. In the autoregulation of nodulation feedback, a signal produced in incipient root nodules induces the production of an inhibitory signal in the shoot; this signal is transported to the root and limits subsequent rhizobial infection and nodulation (Limpens and Bisseling, 2003; Searle et al., 2003; Ferguson et al., 2010). The extent of nodulation is also regulated by the nitrate content in the soil (Gibson and Harper, 1985; Imsande, 1986; Streeter, 1988). Thus, disparities in the carbon/nitrogen balance or a decline in the nitrogen demand may result in decreased photosynthate supply from shoot to nodules, arresting their growth and development (Bacanamwo and Harper, 1996, 1997).

The trehalose biosynthetic pathway functions as a major regulator of carbon metabolism and thus plays a fundamental role in plant growth and development (Wahl et al., 2013; Lunn et al., 2014; Figueroa et al., 2016; Figueroa and Lunn, 2016). Trehalose, a non-reducing glucose disaccharide, occurs widely in nature. The most common route for trehalose biosynthesis involves transfer of UDP-glucose to glucose-6-phosphate by the enzyme trehalose-6-phosphate synthase (TPS) to form trehalose-6-phosphate. Dephosphorylation of trehalose-6-phosphate by trehalose-6-phosphate phosphatase (TPP) yields free trehalose. In plants, multi-gene families encode TPS and TPP (Leyman et al., 2001). *TPS* genes include Class I genes, which usually encode catalytically active TPS enzymes, and Class II genes, which encode proteins that do not possess TPS or TPP enzymatic activity but contain TPS and TPP domains (Avonce et al., 2010). The Class III family encodes functional TPP enzymes (Vogel et al., 1998; Vandesteene et al., 2012). The catabolism of trehalose is mediated by the enzyme trehalase (Van Houtte et al., 2013).

Interestingly, various microorganisms, including rhizobia, produce trehalose during their symbiotic or pathogenic interactions with plants (Brodmann et al., 2002; Foster et al., 2003; Ocón et al., 2007; Wilson et al., 2007, 2010; Nehls, 2008; Barraza et al., 2013; Garg and Singla, 2016). Free-living rhizobia under physiological stress produce high levels of trehalose and this metabolite plays an important role as osmoprotectant in the development of symbiotic nitrogen-fixing root nodules (Sugawara et al., 2010) or during nodule senescence (Müller et al., 2001). Although, most of the trehalose in nitrogen-fixing nodules is produced by the symbiotic bacteria (Suárez et al., 2008; López et al., 2009), increases of diverse trehalose-related transcripts have been reported in other tissues of legume plants living in symbiosis with rhizobia (Pontius et al., 2003; Ramírez et al., 2005; Hernández et al., 2007; Thibivilliers et al., 2009; O'Rourke et al., 2014).

Previously, we studied the effect of modifying the endogenous expression levels of trehalase (*PvTRE1*) in composite common bean plants. Diminishing the transcript levels of *PvTRE1* in transgenic nodules results in increased trehalose contents and substantially improves the nitrogen-fixation rate without affecting plant performance (Barraza et al., 2013). In this work, we silenced the expression of a Class II *TPS* gene (*PvTPS9*) in nodules of common bean elicited by *Rhizobium etli* strain CFN42, and observed important systemic modifications in the expression of all Class II *TPS* genes as well as in the final contents

of trehalose. Interestingly, although neither nodule number nor nitrogen fixation rates were altered, plant biomass was severely reduced. Altogether, the deleterious effects observed in composite common bean plants caused by reducing the expression of *PvTPS9* in root nodules suggest that *PvTPS9* plays an important role in modulating trehalose metabolism in the symbiotic nodule and, therefore, throughout the plant.

MATERIALS AND METHODS

Plant Materials and Growth Conditions

Phaseolus vulgaris cv. Negro Jamapa (common bean) composite plants were used in this study. The generation of composite common bean plants was achieved following the protocol published by Estrada-Navarrete et al. (2007). Common bean seeds were surface disinfected and germinated under sterile conditions for 2 days and then transferred to pots with vermiculite. Plantlets were grown in a greenhouse under natural photoperiod and 26–28°C temperature, and watered with Broughton & Dilworth (B&D) nutrient solution (Broughton and Dilworth, 1971). Hairy roots of 3- to 6-cm emerging from the cotyledonary node of common bean seedlings infected with *Agrobacterium rhizogenes* strain K599 were obtained after 2 weeks. Transgenic roots were identified by epifluorescence microscopy following the signal emitted by the reporter gene [encoding Tomato Fluorescent Protein (Tdt), Valdés-López et al., 2008]. Wild-type and untransformed roots were excised and the composite plants were planted in new pots containing fresh vermiculite. Immediately afterwards, transformed roots were directly inoculated by adding 1 mL of 5×10^8 mL⁻¹ *R. etli* strain CFN42 culture, and grown for 21 d. Composite bean plants were regularly watered with a B&D nitrogen-free nutrient solution (without the addition of KNO₃). Transgenic roots and nodules were collected in liquid nitrogen, finely ground with a mortar and pestle and stored at -80°C until they were used for quantitative RT-PCR (qRT-PCR) and carbohydrate profile analysis by high-performance liquid chromatography (HPLC). Alternatively, transgenic nodules were collected, formaldehyde-fixed, and embedded in LR-White for detailed characterization by optical and confocal microscopy, and also by transmission electron microscopy (TEM).

In silico Identification of the Trehalose-6-Phosphate Synthase Gene Families in Common Bean and Phylogenetic Analysis

We identified expressed sequence tags (ESTs) corresponding to a *Trehalose-6-Phosphate Synthase (TPS)* gene expressed in common bean nodules (Ramírez et al., 2005; Hernández et al., 2007), which is presumably involved in the biosynthesis of trehalose, using the common bean Gene Index v.4.0 (DFCI, <http://compbio.dfci.harvard.edu/tgi/>). In addition, by analyzing the whole common bean genome (Phytozome v11, <http://www.phytozome.net/>; Mazorka, <http://mazorka.langebio.cinvestav.mx/blast/>), we identified the complete coding sequence of seven *TPS*-paralogous genes.

The coding sequences of these putative TPS genes were analyzed with Pfam (<http://pfam.xfam.org>), and then analyzed by BLAST with other TPS sequences deposited in GenBank using the BLASTX tool at the National Center for Biotechnology Information (NCBI, <https://blast.ncbi.nlm.nih.gov>) website. Multiple sequence alignment of the full-length TPS protein sequences was performed using ClustalX 1.83 (Thompson et al., 1997) and manually edited using Seaview (Galtier et al., 1996).

Phylogenetic trees were generated using MrBayes 3 (Ronquist and Huelsenbeck, 2003) and PhyML 3.0 (Guindon et al., 2010). In the first run of MrBayes3, all available fixed-rate amino acid substitution models were explored, clearly showing the Whelan and Goldman model produced the best fit for the data. In a second iteration, the program was executed in two independent runs with six chains for 7500 generations using the Jones-Taylor-Thornton model. Although, the phylogenetic trees were sampled every 100 generations, the first 500 were discarded. The remaining 7000 were used to build a consensus phylogenetic tree that allowed calculation of the posterior probability of all bipartitions. PhyML 3.0 is designed to calculate maximum likelihood phylogenies for large data sets using a Hill-Climbing algorithm. This program was run with 100 bootstraps and the Jones-Taylor-Thornton substitution model was used.

Molecular Chimeras and Plant Transformation

The 3'-untranslated region (3'-UTR) of *PvTPS9* (300 bp, **Figure S1**) was amplified by PCR from complementary DNA (cDNA) synthesized from total RNA obtained from 21 days post-inoculation (dpi)- root nodules elicited with *R. etli* strain CFN42. DNA amplification was achieved using a combination of *PvTPS9*RiFwd and *PvTPS9*RiRev primers (**Table S1**, **Figure S1**). The resulting 300-bp DNA fragment was cloned into pENTR/SD/D-TOPO (Invitrogen, Carlsbad, CA, U.S.A.) and later recombined into the pTdT-DC-RNAi binary vector (Valdés-López et al., 2008). The orientation of the inserted 3'UTR of *PvTPS9* in this vector was confirmed by PCR using the WRKY-5-Rev and *PvTPS9*RiFwd primers (**Table S1**). The open reading frame of the *otsA* gene was obtained by amplification with PCR using genomic DNA from *R. etli* as template and a combination of *ReTPS*For and *ReTPS*Rev primers (**Table S1**). The resulting 1.4 Kb DNA fragment was cloned into pCAMBIA-1304 vector to produced the p35S::*ReTPS* molecular construct. The procedure to generate the *PvTRE1*-RNAi plasmid has been described by Barraza et al. (2013). Plasmids were introduced by electroporation into *A. rhizogenes* strain K599, and used for plant transformation as described.

Bacterial Strains and Cultures

R. etli strain CFN42 was grown in peptone-yeast extract (PY) liquid culture [0.5% bacto-peptone (w/v), 0.3% yeast extract (w/v), 7 mM CaCl₂·2H₂O] supplemented with 20 µg/mL nalidixic acid at 30°C to a cell density of 5×10^8 mL⁻¹. *A. rhizogenes* K599 was grown in LB solid culture at 30°C for 24 h. *A. rhizogenes* K599 transformed with pTdT-DC-RNAi, *A. rhizogenes* K599 with pTdT-GUS-RNAi, and *A. rhizogenes* K599 with pTdT-*PvTPS9*-RNAi were grown in LB solid culture supplemented with 200

µg/mL spectinomycin at 30°C for 24 h. All these *A. rhizogenes* K599 strains were used to generate composite common bean plants.

In silico Identification of PvmiR172 in Common Bean

The microRNA172 (miRNA172) was previously identified in leguminous plants (Lu and Yang, 2010; Peláez et al., 2012). Its presence in common bean was confirmed by analyzing the whole *Phaseolus vulgaris* genome (Phytozome v11, <http://www.phytozome.net>; Mazorka, <http://mazorka.langebio.cinvestav.mx/blast/>), and the retrieved sequence of *PvmiR172* was later analyzed in miRBase (<http://www.mirbase.org/search.shtml>).

TEM and Optical Microscopy

Nodules at 21 dpi (9 nodules per experiment collected from different composite bean plants) were embedded in LR-White resin after being fixed with 2% *p*-formaldehyde and 0.4% glutaraldehyde in PBS buffer for 2 h at room temperature, and subjected to dehydration in a graded ethanol series. For optical microscopy, tissue sections of 7 µm were stained with toluidine blue. The optical microscopy analyses were performed with a light microscope (Motic BA300, Xiamen, China) and photographed with a digital camera (Motic M1000, Xiamen, China). Samples for transmission electron microscopy (TEM) were stained with uranyl acetate. Thin sections of 60 nm were prepared with an ultramicrotome (Leica Ultracut R) and stained with uranyl acetate. TEM analyses were performed with a Zeiss EM900 transmission electron microscope dual vision coupled cam system (Gatan, Inc., Pleasanton, CA, U.S.A.).

Culture of Rhizobium Re-Isolated from Transgenic Nodules and Determination of Colony Forming Units

Nodules at 21 dpi (9 nodules per experiment collected from different composite bean plants) were surface-disinfected by immersion in sodium-hypochlorite (10% v/v) for 10 min. Then, each nodule was homogenized in 5 volumes of 100 mM MgCl₂ using a plastic pipette. For each nodule, 100 µL of a serial dilution (10⁰–10⁻⁸) were plated onto PY solid medium supplemented with 20 µg/mL nalidixic acid and incubated for 24 h at 30°C. Later, *R. etli* CFN42 colony-forming units were determined.

Analysis of the Carbohydrate Profile of Composite Common Bean Plants by High-Performance Liquid Chromatography

Nodules and leaves from composite common bean plants harvested 21 dpi were collected, weighed, frozen in liquid nitrogen, and finely ground. Samples were mixed with 1 mL 80% ethanol (v/v) for 10 min at 80°C. The supernatant was dried, dissolved in 1 mL HPLC grade water, and filtered through a 0.22-µm membrane to remove impurities. These extracts were analyzed by high-performance liquid chromatography (HPLC) in a Waters-600E system controller (Waters, Milford, MA, U.S.A.) equipped with a Waters 410 refractive index

detector (Waters, Milford, MA, U.S.A.) and a carbohydrate analysis column (Kromasil NH₂-5 mm, Supelco, St. Louis, MO, U.S.A.). The temperature of the column was kept at 35°C during the analysis. The mobile phase used in these assays was acetonitrile:water (80:20) at a flow rate of 1.2 mL/min. Glucose, fructose, sucrose, maltose, and trehalose (Sigma-Aldrich) standard solutions were used as reference points. Standard curves used to carry out the quantifications had a correlation index ranging from 0.987 to 0.993. Results were expressed as $\mu\text{g}/\text{mg}$ of fresh weight.

Efficiency of Symbiotic N₂ Fixation of Transformed Roots

Nitrogen fixation was assayed using the acetylene reduction method (Vessey, 1994). Briefly, 21 dpi transgenic roots inoculated with *R. etli* CFN42 (9 individual roots per experiment) were placed in a 160-mL vial closed with a serum cap. Four milliliters of air was withdrawn from the closed vial and replaced by acetylene gas. Ethylene production was assayed in a gas chromatograph and expressed as nanomoles of ethylene per minute per nodule of fresh weight.

Quantitative PCR Assays

RNA from plant tissues was extracted using TRIzol (Invitrogen, Carlsbad, CA, U.S.A.). RNA quantity was measured spectrophotometrically, and only RNA samples with a 260/280 ratio of between 1.9 and 2.1 and a 260/230 ratio of greater than 2.0 were used. The integrity of RNA samples was confirmed by agarose gel electrophoresis. For reverse transcription, total RNA was treated with DNaseI (Invitrogen), and transcribed using the Revert Aid H Minus First-strand cDNA synthesis kit (Fermentas) with anchored-oligo (dT)₁₈ primer, according to the manufacturer's instructions. For qRT-PCR analysis, a LightCycler480 Real-time PCR system (Roche, Penzberg, Germany) was used. qRT-PCR was performed according to the Maxima SYBR Green qPCR Master Mix (2X) protocol (Thermo Scientific, Waltham, MA, U.S.A.). A control sample with no DNA was used in each assay. Primers are listed in **Table S1**. In general, qPCR data came from six independent ($n = 6$) experimental replicas. The statistical significance was determined with an unpaired two-tailed Student's *t*-test. Each biological replicate was tested in triplicate and data were normalized to the *Elongation factor 1-alpha* (*PvEF1a*) reference gene (Livak and Schmittgen, 2001).

Common Bean Argonate (*PvAGO1*) Immunoprecipitation Followed by qRT-PCR Analysis

The immunoprecipitation (IP) assays were carried out according to Qi and Mi (2010) with some minor modifications (Contreras-Cubas et al., 2012). Briefly, 80 mg ground tissue from 14 and 22 dpi nodules was homogenized with 1 mL extraction buffer [50 mM Tris-HCl pH 7.5, 1.5 mM NaCl, 0.1% Nonidet 40, 4 mM MgCl₂, 5 mM DTT, 1 tablet/10 mL protease inhibitor (Roche, Penzberg Germany)]. The homogenate was centrifuged to $19,083 \times g$ for 25 min to pellet the cellular debris. The

supernatant was incubated with 5 μL protein A-agarose pearls (Roche, Penzberg Germany) for 1 h at 4°C with constant rotation. Then, this mixture was centrifuged at $250 \times g$ for 5 min to remove nonspecific Protein A-binding proteins. A 1:50 final dilution of anti-*PvAGO1* antibody with 10 μL protein was added to the supernatant and incubated overnight at 4°C with constant rotation. Material bound to the Protein A-agarose pearls was washed with 1 mL extraction buffer three times. Protein complexes bound to the A-agarose pearls (IP samples) were resuspended in 30 μL extraction buffer and treated with TRIzol (Invitrogen, Carlsbad, CA, U.S.A.) for RNA extraction.

The RNA purified from the IP samples was used for cDNA synthesis with the Ncode miRNA First-strand cDNA synthesis kit (Invitrogen, Carlsbad, CA, U.S.A.) according to the manufacturer's recommendations. The Ncode kit is designed to detect the mature form of the miRNA of interest, but not the precursor molecule. To remove DNA, the RNA was treated with DNaseI as indicated (Invitrogen, Carlsbad, CA, U.S.A.). The absence of DNA in these samples was confirmed by a simple PCR assay (preheating for 5 min at 95°C, followed by 40 cycles of denaturing for 15 s at 95°C, annealing and elongation for 15 s at 55.8°C) using Taq-DNA polymerase (Fermentas Life Sciences, Waltham, MA, U.S.A.). cDNA synthesis was performed using the standard First Strand cDNA Synthesis kit (Fermentas) according to the manufacturer's protocol. For qRT-PCR analysis, a LightCycler480 Real-time PCR system (Roche, Penzberg, Germany) was used. The qRT-PCR was performed according to the Maxima SYBR Green qPCR Master Mix (2X) protocol (Thermo Scientific, Waltham, MA, U.S.A.). A control sample with no DNA was used in each assay. The primers are listed in **Table S1**. The miRNAs co-immunoprecipitated with the anti-*PvAGO1* antibody were derived from three independent ($n = 3$) biological replicates. Each biological replicate was tested in triplicate technical replicates and data were normalized to *PvmiR2118* and *PvmiR172* (Arenas-Huertero et al., 2009). The statistical significance of the obtained results was determined with an unpaired two-tailed Student's *t*-test.

RESULTS

Identifying Plant Trehalose Biosynthetic Genes in Nitrogen-Fixing Nodules of Common Bean

We identified 10 genes encoding trehalose-6-phosphate synthases (TPS) and 9 genes encoding trehalose 6-phosphate phosphatases (TPP) in the common bean genome (Phytozome v11, <http://www.phytozome.net>; Mazorka, <http://mazorka.langebio.cinvestav.mx/blast/>). Amino acid sequence comparisons allowed us to classify these proteins into the previously well-established Class I, Class II, and Class III gene families involved in the biosynthesis of trehalose (Leyman et al., 2001; Avonce et al., 2006). The common bean genome encoded three Class I genes (*PvTPS1-PvTPS3*), seven Class II genes (*PvTPS4-PvTPS10*) (**Figure 1A** and **Table S2**), and nine Class III *TPP* genes (*PvTPPA-PvTPPI*) (**Table S2**). Class I gene members were divided in two subgroups that

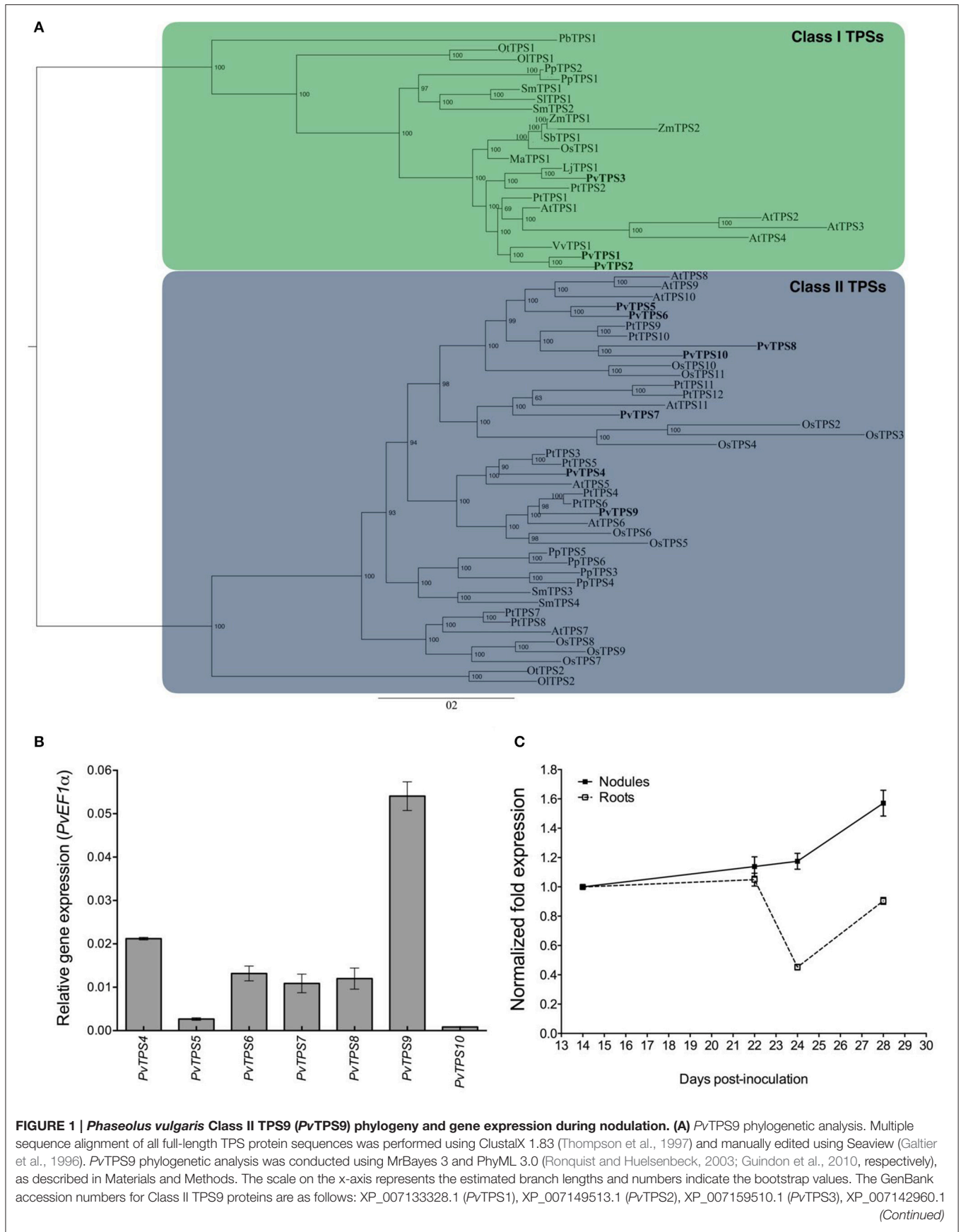


FIGURE 1 | Continued

(PvTPS4), XP_007153644.1 (PvTPS5), XP_007157471.1 (PvTPS6), XP_007154820.1 (PvTPS7), XP_007155406.1 (PvTPS8), XP_007153210.1 (PvTPS9), XP_007138100.1 (PvTPS10). **(B)** Relative expression levels of the *P. vulgaris* Class II TPS-encoding genes in 21 dpi (days post-inoculation) wild-type root nodules elicited by *R. etli* strain CFN42. The qPCR data came from six independent ($n = 6$) wild-type roots, tested in triplicate and normalized to the expression of the *Elongation factor 1-alpha (PvEF1a)* gene. Plotted data represent the expression ratio and are shown as means \pm SD. **(C)** *PvTPS9* gene expression profile during nodule development. qPCR data came from six independent ($n = 6$) biological replicates, tested by technical triplicate and normalized to the expression of the *Elongation factor 1-alpha (PvEF1a)* reference gene. Plotted data represent the expression level of *PvTPS9* in nodules (closed squares) or in nodule-depleted roots (open squares) at different times (dpi), and are shown as means \pm SD.

diverged after the division between monocots and dicots. One subgroup contained only *PvTPS3*, its sequence being closer to *TPS* genes from other legume species such as *Lotus japonicus*; the other subgroup contained *PvTPS1* and *PvTPS2* (**Figure 1A**). As found in other plants, common bean Class II TPS proteins were clustered in subfamilies containing members from both monocots and dicots (**Figure 1A**), suggesting that the Class II TPS of common bean arose from ancient gene duplication events followed by specialization, as has been proposed for *Arabidopsis thaliana* Class II TPS (Ramon et al., 2009; Avonce et al., 2010). *In silico* analysis of the *P. vulgaris* transcriptome (Ramírez et al., 2005; Hernández et al., 2007; DFCL, <http://compbio.dfci.harvard.edu/tgi/>) revealed that all *TPS* and *TPP* genes in common bean plants were expressed, either during some part of plant development or in a tissue-specific manner.

We performed qRT-PCR assays using total RNA obtained from wild-type root nodules at 21 dpi to assess the accumulation of transcripts of common bean *TPS* genes. Results indicate that the *PvTPS9* transcript is the major transcript of the Class II *TPS* family members that accumulated in this organ (**Figure 1B**). Then, we specifically determined the expression profile of *PvTPS9* in roots and in root nodules of common bean plants at 14, 22, 24, and 28 dpi (**Figure 1C**). In nodule-depleted roots, the transcript level of *PvTPS9* remained practically constant from 14 to 22 dpi. However, in root nodules from 22 to 24 dpi, its accumulation decreased by $55 \pm 2\%$, then returned to levels similar to those observed at 14 to 22 dpi. The transcript level of *PvTPS9* did not change in 14 to 24 dpi root nodules, although there was a significant increase from 24 to 28 dpi (**Figure 1C**), suggesting that *PvTPS9* plays an important role during the senescence of the root nodules.

Silencing of *PvTPS9* Diminishes Trehalose Levels and Modifies the Expression of Other Class II *TPS* Family Members in the Symbiotic Nodule

Previous work demonstrated the successful use of RNA interference (RNAi) to silence genes in composite bean plants, which have a wild-type shoot and transgenic roots (Valdés-López et al., 2008; Montiel et al., 2012; Barraza et al., 2013). Here, using the same approach mediated by *Agrobacterium rhizogenes* strain K599, we down-regulated the expression of *PvTPS9* by $85 \pm 1\%$ in 21 dpi transgenic nodules transformed with the pTdT-*PvTPS9*-RNAi construct (**Figure 2A**). In these experiments, nodules formed on hairy roots of common bean

plants induced by untransformed *A. rhizogenes* K599 (used as a control) or by *A. rhizogenes* transformed with the pTdT-DC-RNAi (control nodules with empty vector) had unchanged levels of *PvTPS9* expression (**Figure 2A**).

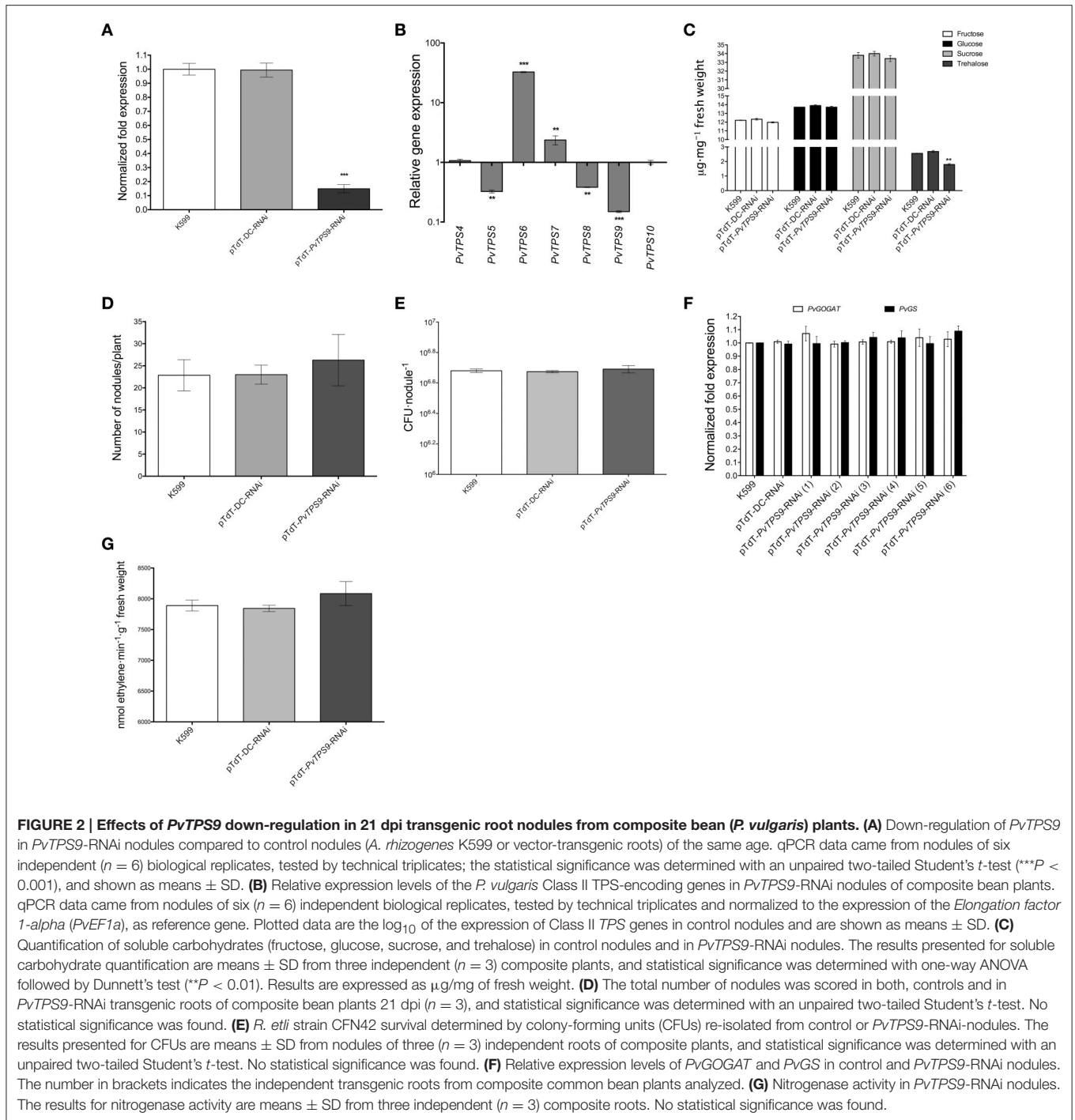
Transcript levels of all Class II *TPS* family members of common bean were determined in pTdT-*PvTPS9*-RNAi 21 dpi transgenic root nodules by qPCR. Compared to control nodules [*A. rhizogenes* K599 or *A. rhizogenes* K599 transformed with the empty vector (pTd-DC-RNAi)], accumulation of *PvTPS9* transcript was reduced by 7-fold (**Figure 2B**). In these plants, the accumulation of *PvTPS6* and *PvTPS7* transcripts also decreased, by 33- and 2-fold, respectively, while *PvTPS4* and *PvTPS10* decreased by 3-fold (**Figure 2B**). *PvTPS1* and *PvTPS7* were the only members of this gene family for which expression was not altered (**Figure 2B**). However, in *PvTPS9* down-regulated nodules, the trehalose content declined up to $30 \pm 3\%$ (**Figure 2C**), which did not affect the final number of nodules (**Figure 2D**) or the number of bacteroids within these nodules (**Figure 2E**).

Interestingly, neither the silencing of *PvTPS9* or the changes in expression of other Class II *TPS* genes in root nodules modified their capacity to fix nitrogen, as deduced from the unaltered expression of the transcripts corresponding to two key enzymes involved in this process, NADH-Glutamate Synthase II (*PvGOGAT*) and Glutamine Synthetase (*PvGS*) (**Figure 2F**), as well as by the acetylene gas reduction rate (**Figure 2G**) observed in *PvTPS9* down-regulated nodules versus control nodules.

Together, these data suggest that directly or indirectly *PvTPS9* modulates trehalose levels in the nodule, but does not interfere with the nitrogen-fixation process.

Silencing of *PvTPS9* in Composite Common Bean Roots Dramatically Affects Nodule Morphology and Bacteroid Size

Determinate common bean root nodules consist of three major tissues: a central infection zone (mainly composed by infected and uninfected cells), an inner cortex that includes vascular bundles, and an outer cortex. All of our silenced and control plants produced similar final numbers of viable bacteroids within the nodules (**Figure 2E**), and similar numbers of nodules per plant (**Figure 2D**). By contrast, the nodule size in pTdT-*PvTPS9*-RNAi nodules dramatically increased ($44 \pm 4\%$, **Figures 3A,B**). Detailed observations of nodule sections stained with toluidine blue (**Figures 3D,E**) indicated a notable increase in the thickness of the cell wall in both infected and uninfected cells (**Figure 3E**) compared to controls (**Figure 3D**). Moreover, both infected

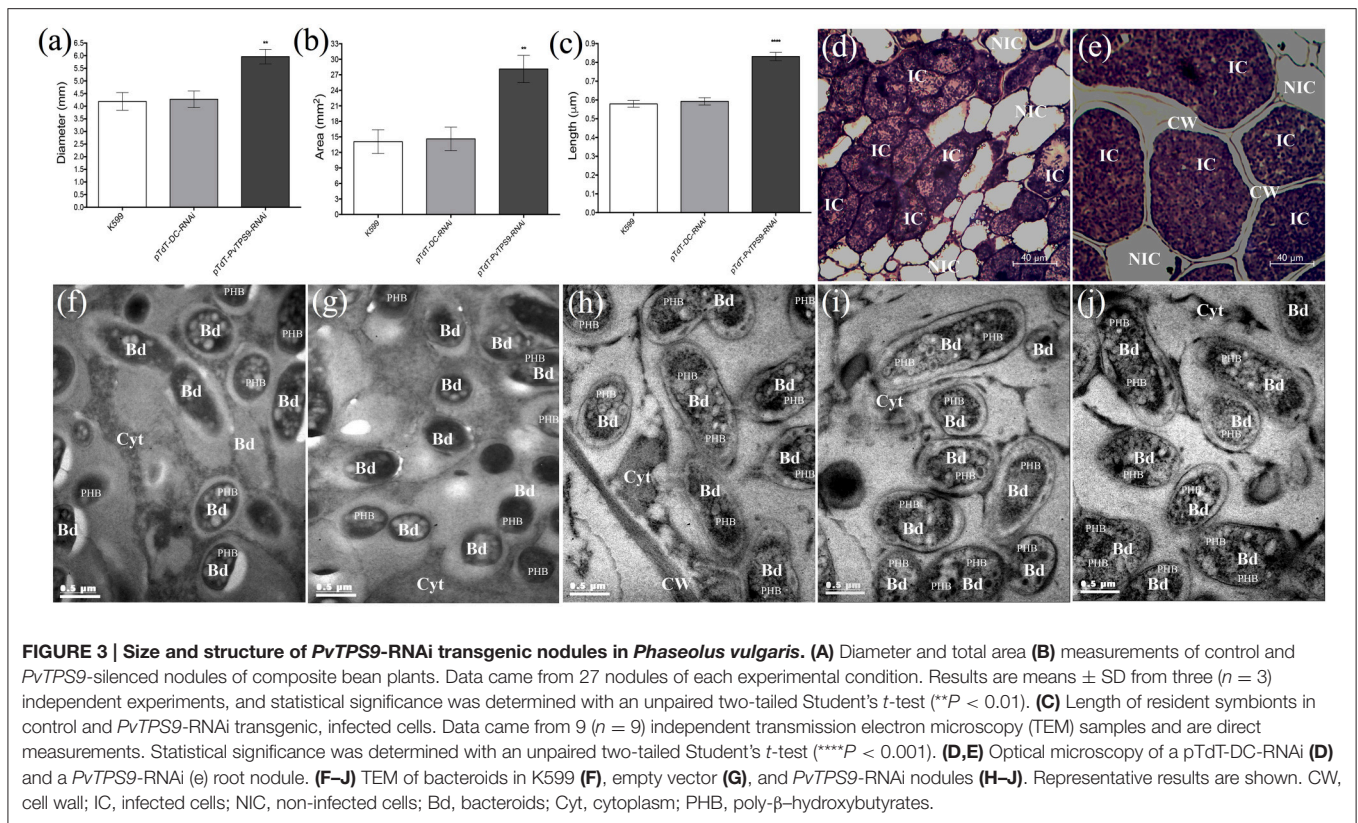


and uninfected cells of pTdt-*PvTPS9*-RNAi nodules (Figure 3E) were larger than the cells in control nodules (Figure 3D).

Ultra-thin sections of 21 dpi pTdt-*PvTPS9*-RNAi transgenic nodules as well as nodules from control roots (*A. rhizogenes* strain K599 and empty vector) were analyzed by transmission electron microscopy (TEM, Figures 3E,J). Compared to controls (Figures 3E,G,C), bacteroids contained in pTdt-*PvTPS9*-RNAi nodules were considerably larger (Figures 3H,J,C).

These bacteroids accumulated higher amounts of poly- β -hydroxybutyrate (PHB) in the cytoplasm (Figures 3E,G compared to Figures 3H-J), a carbon polymer product of glucose or starch assimilation employed by rhizobia as an energy storage molecule that can be metabolized when other common energy sources are not available.

As the plant carbohydrate supply has been proposed to regulate nodule development, we explored whether differences



in the soluble carbohydrate content of *PvTPS9*-RNAi and control nodules could explain the morphological variations observed in pTdt-*PvTPS9*-RNAi nodules. Remarkably, only trehalose showed a significant reduction in *PvTPS9*-RNAi nodules compared to controls.

Silencing *PvTPS9* in Root Nodules Produces a Deleterious, Systemic Effect in Composite Bean Plants

In pTdt-*PvTPS9*-RNAi composite common bean plants inoculated with *R. etli* strain CFN42, we observed a clear reduction in leaf size compared to inoculated controls (Figure S2). We quantified the leaf area (Figure 4A) and the leaf biomass (Figures 4B,C) in these plants, and found reductions of $36 \pm 3\%$ and $36 \pm 5\%$, respectively. However, the foliage of pTdt-*PvTPS9*-RNAi composite bean plants did not show chlorosis (Figure S2), a common symptom in plants subjected to environmental stresses. The reduction in leaf size of pTdt-*PvTPS9*-RNAi composite common bean plants was not caused by water deficit, based on comparisons of the relative water content of pTdt-*PvTPS9*-RNAi- and control plants (Figure 4D).

Remarkably, analysis of the trehalose content in leaves of pTdt-*PvTPS9*-RNAi composite plants indicated a 30% reduction of this carbohydrate compared to control plants (Figure 4E), similar to that observed in root nodules (Figure 2C). Unexpectedly, other soluble sugars such as sucrose, glucose and

fructose, did not show any change (Figure 4E). It has been reported that Class II TPS gene expression responds to carbon availability in *A. thaliana* (Ramon et al., 2009). Accordingly, we determined the transcript levels of the common bean Class II TPS gene family members, and found that *PvTPS4*, *PvTPS5*, and *PvTPS8* were up-regulated by 4-fold, 1-fold, and 3-fold, respectively (Figure 4F), whereas *PvTPS7* and *PvTPS9* were down-regulated by 2.1-fold and 1.2-fold (Figure 4F). The remaining Class II TPS gene family members, *PvTPS6* and *PvTPS10*, did not significantly change in expression (Figure 4F).

DISCUSSION

In this work we used an *in silico* approach to identify trehalose biosynthesis-related genes in the genome of common bean (*P. vulgaris* L.) and found 10 TPS- and 9 TPP-encoding genes (Table S2). A similar number is found in other plant species (Avonce et al., 2010; Vandesteene et al., 2012). In *P. vulgaris*, three of the TPS genes belong to Class I (*PvTPS1-3*), whereas the other seven belong to Class II (*PvTPS4-10*) (Table S2). As in *A. thaliana*, phylogenetic analysis of the TPS genes of common bean revealed pairs of paralogous loci, such as *PvTPS1* and *PvTPS2*, *PvTPS5* and *PvTPS6*, or *PvTPS8*, and *PvTPS10*. These paralogs have been proposed to be the result of a recent whole-genome duplication event (Figure 1A). By contrast, other genes, like *PvTPS9* or *PvTPS7*, are grouped in clades formed by monocot or dicot species (Figure 1A), suggesting their presence in a common

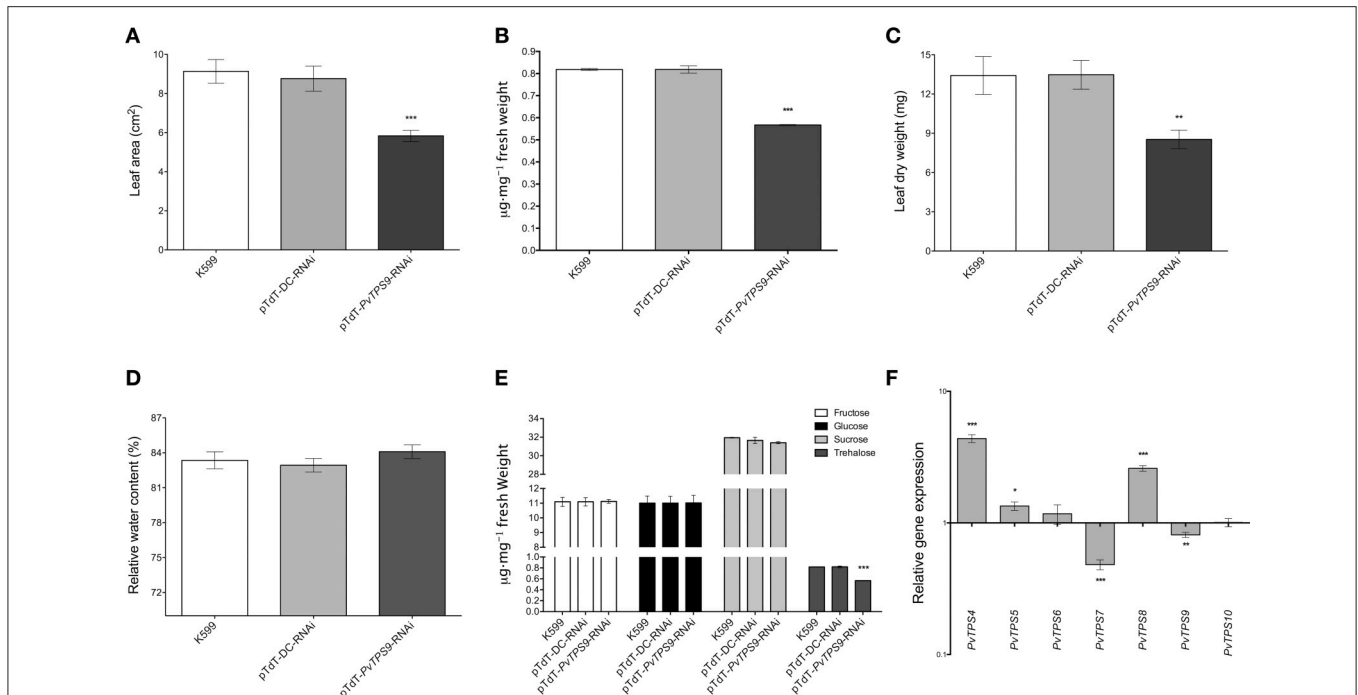


FIGURE 4 | Effect on leaves of *P. vulgaris* PvTPS9-RNAi transgenic roots. (A) Leaf area of composite plants. The results for leaf area are means \pm SD from three independent ($n = 3$) composite plants and statistical significance was determined with an unpaired two-tailed Student's t -test ($***P < 0.001$). **(B)** Trehalose content determination in leaves of PvTPS9-RNAi composite common bean plants. Results are means \pm SD from three independent ($n = 3$) composite plants and statistical significance was determined with an unpaired two-tailed Student's t -test ($***P < 0.001$). **(C)** Leaf biomass determination. Dry leaf weights were obtained from three independent ($n = 3$) composite common bean plants. The results are means \pm SD and statistical analysis was determined with an unpaired two-tailed Student's t -test ($**P < 0.01$). **(D)** Relative water content (RWC) of leaves of composite plants. The results for RWC are means \pm SD from three independent ($n = 3$) composite plants. No statistical significance was found with an unpaired two-tailed Student's t -test. **(E)** Soluble carbohydrate (fructose, glucose, sucrose, and trehalose) quantification in leaves of composite plants. The results presented for soluble carbohydrate quantification in leaves of composite plants are means \pm SD from three independent ($n = 3$) composite plants, and statistical significance was determined with one-way ANOVA followed by Dunnett's test ($***P < 0.001$). **(F)** Relative gene expression levels of the *P. vulgaris* Class II TPS-encoding genes in 21 dpi (days post-inoculation) composite common bean plants. qPCR data came from the foliage of three independent composite plants ($n = 3$) tested by technical triplicate and normalized to the expression of the *Elongation factor 1- α* (*PvEF1a*) gene, and statistical significance was determined with an unpaired two-tailed Student's t -test ($*P < 0.05$; $**P < 0.01$; $***P < 0.001$). Plotted data are expressed as \log_{10} of the relative gene expression of control Class II TPS genes, and are shown as means \pm SD.

ancestor (Avonce et al., 2010; Vandesteene et al., 2012; Schmutz et al., 2014; Vlasova et al., 2016).

In common bean plants, all the TPS genes were expressed either in different tissues or in different developmental stages (Ramírez et al., 2005; Hernández et al., 2007, DFCI, <http://compbio.dfci.harvard.edu/tgi/>). Nevertheless, PvTPS9 was the most abundantly expressed TPS gene in functional nitrogen-fixing root nodules (Figure 1B), a result also seen in other studies (Ramírez et al., 2005; Hernández et al., 2007). Moreover, the PvTPS9 pattern of transcript accumulation during nodule development, compared to its expression in roots (Figure 1C) strongly suggests that PvTPS9 plays an important role in nodule function. Interestingly, several reports have shown that, although Class II TPS proteins contain TPS and TPP domains, they do not possess the corresponding enzymatic activities (Vogel et al., 2001; Ramon et al., 2009; Avonce et al., 2010; Vandesteene et al., 2012; Lunn et al., 2014).

To evaluate the possible role of this protein during root nodule symbiosis, we silenced the expression of PvTPS9 in roots of composite common bean plants infected with *R. etli* strain

CFN42. Compared to controls, PvTPS9-RNAi nodules showed a reduction in PvTPS9 transcript levels below 80% (Figure 2A) and a change in expression of most Class II TPS gene family members (Figure 2B). This variation in gene expression coincided with a significant decrease in the nodule trehalose content (Figure 2C). Class II TPS gene expression responds to carbon availability in *A. thaliana* (Ramon et al., 2009). Our data from PvTPS9-RNAi composite common bean plants, in which the expression of most of the Class II TPS family members has been modified, further indicate that Class II TPS genes could have important roles in carbon allocation.

Remarkably, a similar effect was observed in the foliage of pTdt-PvTPS9-RNAi composite common bean plants inoculated with *R. etli* strain CFN42 (Figures 4E,F), which displayed nearly a 40% reduction in leaf size and leaf biomass compared to controls (Figures 4A–D and Figure S2). This is not the first time that organ-specific manipulation of trehalose metabolism has affected the whole plant. We previously demonstrated that silencing the expression of trehalase (*PvTRE1*) in root nodules of composite common bean plants positively influences the rate of

nitrogen fixation by increasing the number of active bacteroids in transformed nodules by approx. 10-fold, which induces a significant increase in the trehalose content in nodules and in the foliage (Barraza et al., 2013). Trehalose and associated metabolites are important systemic modulators of plant growth and sugar signaling (Gómez et al., 2006, 2010; Schluempmann and Paul, 2009; Wingler et al., 2012; Lunn et al., 2014). Therefore, although we did not observe any change in metabolizable sugars in *PvTPS9*-RNAi composite common plants (Figures 2C, 4E), the reduction of trehalose may be responsible for altering the metabolism of carbon in the whole plant, thus reducing plant growth.

In this work we showed that *PvTPS9*-RNAi nodules, which on average contained 30% less trehalose (Figure 2C), were 33% larger (Figures 3A,B) and displayed important structural modifications, such as the enlargement of both infected and uninfected cells, and a remarkable thickening of the cell wall (Figures 3D,E). Furthermore, resident bacteroids of these organs were considerably larger than their equivalents in control nodules and contained a higher number of poly- β -hydroxybutyrate (PHB) granules in their cytoplasm (Figures 3H–J compared to Figures 3C, F, G). Although, the precise roles of PHB metabolism in the legume-rhizobium symbiosis are not completely understood, experimental evidence indicates that PHB is biosynthesized and turned over rapidly during active nitrogen fixation, and is extremely important for rhizobia to regulate plant carbon flux (Lodwig and Poole, 2003; Trainer et al., 2010). Even though the nitrogen fixation rate in *PvTPS9*-RNAi nodules was not changed (Figure 2G), their altered morphology suggests that the metabolism of trehalose plays a pivotal role in nodule formation and development, and affects the carbon metabolism in rhizobia.

Different lines of evidence suggest that most of the trehalose accumulated in the nodule originates from the bacteria, rather than from the plant (Müller et al., 2001; Suárez et al., 2008; López et al., 2009; Vaclare et al., 2010). Thus, the changes observed in the concentration of trehalose in composite *PvTPS9*-RNAi and control plants could be explained by an adjustment in the biosynthesis of trehalose by rhizobia in response to changes in the carbon metabolism of the plant caused by variations in the expression of the plant Class II TPS genes. Although, *PvTPS9* encodes a Class II TPS, a well-known non-catalytically active TPS or TPP protein (Ramon et al., 2009; Vandesteene et al., 2012; Lunn et al., 2014), our data indicate that *PvTPS9* plays a role in the regulation of trehalose metabolism in the symbiotic nodule and in consequence, of the whole plant.

VuTPS6, a Class II TPS gene from *Vigna unguiculata*, has been reported to be regulated by the miRNA *VumiR172b* (Lu and Yang, 2010). Interestingly, *PvmiR172*, a homolog of *VumiR172*, is abundant during common bean nodulation (Peláez et al., 2012 and Figure S4B of this work). Excitingly, a sequence alignment of *PvmiR172* and the transcript of *PvTPS9*, revealed a possible recognition site in the coding region (Figure S4A). The transcript abundance of the canonical target of miR172, *APETALA2* (*PvAP2*), shows an inverse correlation to that of *PvmiR172* during nodulation, an indication that *PvmiR172* modulates the expression of *PvAP2* in *P. vulgaris* (Mlotshwa

et al., 2006; Glazińska et al., 2009; Wollmann et al., 2010; Grigorova et al., 2011; Zhu and Helliwell, 2011; Varkonyi-Gasic et al., 2012). Here, we found that the *PvTPS9* transcript was associated with *PvAGO1*-complexes from 14 and 22 dpi nodules along with *PvAP2* and *PvmiR172*, despite the fact that 5'-RACE analysis revealed no evidence of processing for the *PvTPS9* transcript (Figure S4C). In contrast to *PvAP2*, however, *PvTPS9* levels showed a direct (rather than inverse) correlation with those of *PvmiR172* (Figure S4B), suggesting there is no direct regulation of *PvTPS9* by *PvmiR172* via mRNA degradation. This miRNA may affect *PvTPS9* by another type of regulation, such as inhibition of translation (Voinnet, 2009; Rügger and Grosshans, 2012). Still, in *p35S::ReTPS* and *PvTRE1*-RNAi transgenic nodules, where the trehalose content increased, we also observed a significant reduction in the *PvmiR172* abundance (Figure S4D). This behavior is opposite to that in *PvTPS9*-RNAi nodules (Figure S5), suggesting that the trehalose content has a direct effect on the abundance of *PvmiR172*. Interestingly, miR172 modulates nodule organogenesis in leguminous plants (Wang et al., 2014; Holt et al., 2015; Nova-Franco et al., 2015).

We also monitored *PvmiR172* and *PvAP2* transcript abundance in the foliage of *PvTPS9*-RNAi composite common bean plants (Figures S3, S5). Here also, the level of *PvmiR172* increased whereas the level of *PvAP2* transcript decreased (Figures S3, S5), supporting the idea that the trehalose content modulates the expression of *PvmiR172* in planta.

In conclusion, we propose that *PvTPS9* plays a key role in modulating trehalose metabolism in the symbiotic nodule and, therefore, in the whole plant. Through such control, *PvTPS9* influences nodule and plant development. Although, we found no evidence for direct regulation of *PvTPS9* by *PvmiR172*, the fact that the trehalose content in symbiotic nodules alters *PvmiR172* abundance strongly suggests that *PvTPS9* is indirectly involved in regulating *PvmiR172* expression. It is tempting to speculate that *PvmiR172* regulates *PvTPS9* through translation inhibition, forming a feedback regulatory loop.

AUTHOR CONTRIBUTIONS

AB was responsible for the experimental work and made substantial contributions to conceptualization and design of the study. Furthermore, he was involved in drafting the manuscript. CC, GE, MV, and JR made substantial contributions to the experimental work. JR, NA, CQ, FS, and CD made substantial contributions to conceptualization and design of the study and were involved in drafting the manuscript and revising it critically for important intellectual content. FS and CD contributed reagents/materials/analysis and CQ and CD gave final approval for the version to be published.

FUNDING

AB was supported by a PhD scholarship (169219) from Consejo Nacional de Ciencia y Tecnología (CONACYT)-México. This research was partially supported by grants from CONACYT-México (No. 177207) and from the Universidad Nacional

Autónoma de México (Dirección General Asuntos del Personal Académico PAPIIT No. IN206815) to CD.

ACKNOWLEDGMENTS

We thank Guadalupe Zavala and Xóchitl Alvarado-Affantranger for technical advice, the Laboratorio Nacional de Microscopía Avanzada (LNMA) at the Instituto de Biotecnología of the Universidad Nacional Autónoma de México for the use of equipment, and Paul Gaytán, Jorge Yañez and Eugenio López for primer synthesis and DNA sequencing (Unidad de Síntesis y Secuenciación de ADN at the Instituto de Biotecnología). All authors are grateful to Jennifer M. Mach and Nancy R. Hofmann at Plant Editors (www.planteditors.com) for their detailed and professional editing of this manuscript.

SUPPLEMENTARY MATERIAL

The Supplementary Material for this article can be found online at: <http://journal.frontiersin.org/article/10.3389/fpls.2016.01589/full#supplementary-material>

Figure S1 | Schematic representation of the PvTPS9 cDNA sequence. The coding sequence (CDS) and the 3' untranslated region is shown in white boxes, and the DNA fragment amplified by qPCR and the target region to be silenced by RNAi are shown in green and red boxes, respectively. We also indicate the primer sequence and position to measure PvTPS9 transcript abundance by qPCR and to amplify the 300 bp DNA sequence used in our RNAi design.

Figure S2 | Control (*A. rhizogenes* K599) or PvTPS9-RNAi composite bean plants. Photograph was taken at 21 dpi.

REFERENCES

- Arenas-Huertero, C., Pérez, B., Rabanal, F., Blanco-Melo, D., De la Rosa, C., Estrada-Navarrete, G., et al. (2009). Conserved and novel miRNAs in the legume *Phaseolus vulgaris* in response to stress. *Plant Mol. Biol.* 70, 385–401. doi: 10.1007/s11103-009-9480-3
- Avonce, N., Mendoza-Vargas, A., Morett, E., and Iturriaga, G. (2006). Insights on the evolution of trehalose biosynthesis. *BMC Evol. Biol.* 6:109. doi: 10.1186/1471-2148-6-109
- Avonce, N., Wuyts, J., Verschooten, K., Vandesteene, L., and Van Dijck, P. (2010). The Cytophaga hutchinsonii ChTPSP: first characterized bifunctional TPS-TPP protein as putative ancestor of all eukaryotic trehalose biosynthesis proteins. *Mol. Biol. Evol.* 27, 359–369. doi: 10.1093/molbev/msp241
- Bacanamwo, M., and Harper, J. E. (1996). Regulation of nitrogenase activity in *Bradyrhizobium japonicum*/soybean symbiosis by plant N status as determined by shoot C:N ratio. *Physiol. Plant.* 98, 529–538. doi: 10.1111/j.1399-3054.1996.tb05708.x
- Bacanamwo, M., and Harper, J. E. (1997). The feedback mechanism of nitrate inhibition of nitrogenase activity in soybean may involve asparagine and/or products of its metabolism. *Physiol. Plant.* 100, 371–377. doi: 10.1111/j.1399-3054.1997.tb04795.x
- Barraza, A., Estrada-Navarrete, G., Rodriguez-Alegria, M.-E., Lopez-Munguia, A., Merino, E., Quinto, C., et al. (2013). Down-regulation of PvTRE1 enhances nodule biomass and bacteroid number in the common bean. *New Phytol.* 197, 194–206. doi: 10.1111/nph.12002
- Brodmann, D., Schuller, A., Ludwig-Müller, J., Aeschbacher, R. A., Wiemken, A., Boller, T., et al. (2002). Induction of trehalase in Arabidopsis plants infected with the trehalose-producing pathogen *Plasmodiophora brassicae*. *Mol. Plant-Microbe Interact.* 15, 693–700. doi: 10.1094/MPMI.2002.15.7.693

Figure S3 | PvmiR172, PvAP2, and PvTPS9 transcript abundance determined in the different tissues of common bean plants by qPCR assays. Data came from plant tissues (roots, nodules, leaves, seeds and pods) of six independent ($n = 6$) biological replicates and shown as means \pm SD.

Figure S4 | PvmiR172 expression could be regulated systemically by the trehalose content in *P. vulgaris* plants. (A) Schematic representation of the transcript sequence of PvTPS9 and the putative interaction with PvmiR172, showing three mismatches near the central zone of PvTPS9. (B) PvmiR172 (circles), PvAP2 (triangles), PvTPS9 (squares) gene expression profile during nodule development. qPCR data came from six independent ($n = 6$) wild-type nodules, tested by triplicate and normalized to the expression level of the *Elongation factor 1-alpha* (*PvEF1a*) gene. Plotted data are shown as mean \pm SD. (C) Anti-PvAGO1 RNA co-immunoprecipitation (IP). Total extracts of 14 or 21 dpi wild-type nodules were divided in four parts and used for anti-PvAGO1 immunoprecipitation followed by RNA extraction and cDNA synthesis. qPCR data came from three ($n = 3$) independent experimental replicas tested by triplicate and normalized to the PvmiR2118 reference gene (Livak and Schmittgen, 2001). (D) PvmiR172 abundance and trehalose content in control (*A. rhizogenes* K599) or in p35S::*ReTPS*, *PvTPS9*-RNAi and *PvTRE1*-RNAi transgenic nodules of composite bean plants. qPCR data came from nodules of six independent ($n = 6$) transgenic roots. The statistical significance was determined with an unpaired two-tailed Student's *t*-test (* $P < 0.05$, ** $P < 0.01$, *** $P < 0.001$), and shown as means \pm SD.

Figure S5 | PvmiR172 and PvAP2 transcript abundance in leaves of PvTPS9-RNAi composite common bean plants by qPCR assays. (A,B) Statistical significance was determined with an unpaired two-tailed Student's *t*-test (* $P < 0.05$; *** $P < 0.001$). Plotted data are expressed as \log_{10} of relative gene expression of Class II TPS genes in the control composite common bean plants and shown as means \pm SD.

Table S1 | List of primers used in this work.

Table S2 | Class I, Class II, and Class III gene families involved in the biosynthesis of trehalose in common bean (Phytozome v11, <http://www.phytozome.net>; Mazorka, <http://mazorka.langebio.cinvestav.mx/blast/>).

- Broughton, W. J., and Dilworth, M. J. (1971). Control of leghaemoglobin synthesis in snake beans. *Biochem. J.* 125, 1075–1080. doi: 10.1042/bj1251075
- Contreras-Cubas, C., Rabanal, F. A., Arenas-Huertero, C., Ortiz, M. A., Covarrubias, A. A., and Reyes, J. L. (2012). The *Phaseolus vulgaris* miR159a precursor encodes a second differentially expressed microRNA. *Plant Mol. Biol.* 80, 103–115. doi: 10.1007/s11103-011-9847-0
- Estrada-Navarrete, G., Alvarado-Affantranger, X., Olivares, J.-E., Guillén, G., Díaz-Camino, C., Campos, F., et al. (2007). Fast, efficient and reproducible genetic transformation of *Phaseolus* spp. By *Agrobacterium rhizogenes*. *Nat. Protoc.* 2, 1819–1824. doi: 10.1038/nprot.2007.259
- Ferguson, B. J., Indrasumunar, A., Hayashi, S., Lin, M.-H., Lin, Y.-H., Reid, D. E., et al. (2010). Molecular analysis of legume nodule development and autoregulation. *J. Integr. Plant Biol.* 52, 61–76. doi: 10.1111/j.1744-7909.2010.00899.x
- Figueroa, C. M., Feil, R., Ishihara, H., Watanabe, M., Kölling, K., Krause, U., et al. (2016). Trehalose 6-phosphate coordinates organic and amino acid metabolism with carbon availability. *Plant J.* 85, 410–423. doi: 10.1111/tpj.13114
- Figueroa, C. M., and Lunn, J. E. (2016). A tale of two sugars: trehalose 6-phosphate and sucrose. *Plant Physiol.* 172, 7–27. doi: 10.1104/pp.16.00417
- Foster, A. J., Jenkinson, J. M., and Talbot, N. J. (2003). Trehalose synthesis and metabolism are required at different stages of plant infection by *Magnaporthe grisea*. *EMBO J.* 22, 225–235. doi: 10.1093/emboj/cdg018
- Gage, D. J. (2004). Invasion and infection of roots by symbiotic, nitrogen-fixing rhizobia during nodulation of temperate legumes. *Microbiol. Mol. Biol. Rev.* 68, 280–300. doi: 10.1128/MMBR.68.2.280-300.2004
- Galtier, N., Gouy, M., and Gautier, C. (1996). SEAVIEW and PHYLO_WIN: two graphic tools for sequence alignment and molecular phylogeny. *Comput. Appl. Biosci.* 12, 543–548. doi: 10.1093/bioinformatics/12.6.543

- Garg, N., and Singla, P. (2016). Stimulation of nitrogen fixation and trehalose biosynthesis by naringenin (Nar) and arbuscular mycorrhiza (AM) in chickpea under salinity stress. *Plant Growth Regul.* 80, 5–22. doi: 10.1007/s10725-016-0146-2
- Gibson, A. H., and Harper, J. E. (1985). Nitrate effect on nodulation of soybean by *Bradyrhizobium japonicum*. *Crop Sci.* 25, 497–501. doi: 10.2135/cropsci1985.0011183X002500030015x
- Glazińska, P., Zienkiewicz, A., Wocjciechowski, W., and Kopcewicz, J. (2009). The putative miR172 target gene InAPETALA2-like is involved in the photoperiodic flower induction of *Ipomea nil*. *J. Plant Physiol.* 166, 1801–1813. doi: 10.1016/j.jplph.2009.05.011
- Gómez, L. D., Baud, S., Gilday, A., Li, Y., and Graham, I. A. (2006). Delayed embryo development in the ARABIDOPSIS TREHALOSE-6-PHOSPHATE SYNTHASE 1 mutant is associated with altered cell wall structure, decreased cell division and starch accumulation. *Plant J.* 46, 69–84. doi: 10.1111/j.1365-313X.2006.02662.x
- Gómez, L. D., Gilday, A., Feil, R., Lunn, J. E., and Graham, I. A. (2010). AtTPS1-mediated trehalose 6-phosphate synthesis is essential for embryogenic and vegetative growth and responsiveness to ABA in germinating seeds and stomatal guard cells. *Plant J.* 64, 1–13. doi: 10.1111/j.1365-313x.2010.04312.x
- Grigorova, B., Mara, C., Hollender, C., Sijacic, P., Chen, X., and Liu, Z. (2011). LEUNIG and SEUSS co-repressors regulate miR172 expression in Arabidopsis flowers. *Development* 138, 2451–2456. doi: 10.1242/dev.058362
- Guindon, S., Dufayard, J. F., Lefort, V., Anisimova, M., Hordijk, W., and Gascuel, O. (2010). New algorithms and methods to estimate maximum-likelihood phylogenies: assessing the performance of PhyML 3.0. *Syst. Biol.* 59, 307–321. doi: 10.1093/sysbio/syq010
- Hernández, G., Ramírez, M., Valdes-López, O., Tesfaye, M., Graham, M. A., Czechowski, T., et al. (2007). Phosphorus stress in common bean: root transcript and metabolic responses. *Plant Physiol.* 144, 752–767. doi: 10.1104/pp.107.096958
- Holt, D. B., Gupta, V., Meyer, D., Abel, N. B., Andersen, S. U., Stougaard, J., et al. (2015). micro RNA 172 (miR172) signals epidermal infection and is expressed in cells primed for bacterial invasion in *Lotus japonicus* roots and nodules. *New Phytol.* 208, 241–256. doi: 10.1111/nph.13445
- Immsand, J. (1986). Inhibition of nodule development in soybean by nitrate or reduced nitrogen. *J. Exp. Bot.* 37, 348–355. doi: 10.1093/jxb/37.3.348
- Kouchi, H., Imaizumi-Anraku, H., Hayashi, M., Hakoyama, T., Nakagawa, T., Umehara, Y., et al. (2010). How many peas in a pod? Legume genes responsible for mutualistic symbiosis underground. *Plant Cell Physiol.* 51, 1381–1397. doi: 10.1093/pcp/pcq107
- Leyman, B., Van Dijck, P., and Thevelein, J. M. (2001). An unexpected plethora of trehalose biosynthesis genes in *Arabidopsis thaliana*. *Trends Plant Sci.* 6, 510–513. doi: 10.1016/S1360-1385(01)02125-2
- Limpens, E., and Bisseling, T. (2003). Signaling in symbiosis. *Curr. Opin. Plant Biol.* 6, 343–350. doi: 10.1016/S1369-5266(03)00068-2
- Livak, K. J., and Schmittgen, T. D. (2001). Analysis of relative gene expression data using real-time quantitative PCR and the $2^{-\Delta\Delta CT}$ method. *Methods* 25, 402–408. doi: 10.1006/meth.2001.1262
- Lodwig, E., and Poole, P. (2003). Metabolism of Rhizobium bacteroids. *CRC Crit. Rev. Plant Sci.* 22, 37–78. doi: 10.1080/713610850
- López, M., Tejera, N. A., and Lluch, C. (2009). Validamycin A improves the response of *Medicago truncatula* plants to salt stress by inducing trehalose accumulation in the root nodules. *J. Plant Physiol.* 166, 1218–1222. doi: 10.1016/j.jplph.2008.12.011
- Lu, Y., and Yang, X. (2010). Computational identification of novel microRNAs and their targets in *Vigna unguiculata*. *Comp. Funct. Genomics* 2010:128297. doi: 10.1155/2010/128297
- Lunn, J. E., Delorge, I., Figueroa, C. M., Van Dijck, P., and Stitt, M. (2014). Trehalose metabolism in plants. *Plant J.* 79, 544–567. doi: 10.1111/tpj.12509
- Mlotshwa, S., Yang, Z., Kim, Y., and Chen, X. (2006). Floral patterning defects induced by Arabidopsis APETALA2 and microRNA172 expression in *Nicotiana benthamiana*. *Plant Mol. Biol.* 61, 781–793. doi: 10.1007/s11103-006-0049-0
- Montiel, J., Nava, N., Cárdenas, L., Sánchez-López, R., Arthikala, M. K., Santana, O., et al. (2012). A *Phaseolus vulgaris* NADPH oxidase gene is required for root infection by Rhizobia. *Plant Cell Physiol.* 53, 1751–1767. doi: 10.1093/pcp/pcs120
- Müller, J., Boller, T., and Wiemken, A. (2001). Trehalose becomes the most abundant non-structural carbohydrate during senescence of soybean nodules. *J. Exp. Bot.* 52, 943–947. doi: 10.1093/jxbbot/52.358.943
- Nehls, U. (2008). Mastering ectomycorrhizal symbiosis: the impact of carbohydrates. *J. Exp. Bot.* 59, 1097–1108. doi: 10.1093/jxb/erm334
- Nova-Franco, B., Ñiguez, L. P., Valdés-López, O., Alvarado-Affantranger, X., Leija, A., Fuentes, S. I., et al. (2015). The microRNA172c-APETALA2-1 node as a key regulator of the common bean-Rhizobium etli nitrogen fixation symbiosis. *Plant Physiol.* 168, 273–291. doi: 10.1104/pp.114.255547
- Ocón, A., Hamp, R., and Requena, N. (2007). Trehalose turnover during abiotic stress in arbuscular mycorrhizal fungi. *New Phytol.* 174, 879–891. doi: 10.1111/j.1469-8137.2007.02048.x
- O'Rourke, J. A., Iniguez, L. P., Fu, F., Bucciarelli, B., Miller, S. S., Jackson, S. A., et al. (2014). An RNA-Seq based gene expression atlas of the common bean. *BMC Genomics* 15:866. doi: 10.1186/1471-2164-15-866
- Peláez, P., Trejo, M. S., Ñiguez, L. P., Estrada-Navarrete, G., Covarrubias, A. A., Reyes, J. L., et al. (2012). Identification and characterization of microRNAs in *Phaseolus vulgaris* by high-throughput sequencing. *BMC Genomics* 13:83. doi: 10.1186/1471-2164-13-83
- Pontius, J. U., Wagner, L., and Schuler, G. D. (2003). “UniGene: an unified view of the transcriptome,” in *The NCBI Handbook*, eds J. McEntyre and J. Ostell (Bethesda, MD: National Center for Biotechnology Information), 1–11.
- Qi, Y., and Mi, S. (2010). Purification of Arabidopsis argonaute complexes and associated small RNAs. *Methods Mol. Biol.* 592, 243–254. doi: 10.1007/978-1-60327-005-2_16
- Ramírez, M., Graham, M. A., Blanco-López, L., Silvente, S., Medrano-Soto, A., Blair, M. W., et al. (2005). Sequencing and analysis of common bean ESTs. Building a foundation for functional genomics. *Plant Physiol.* 137, 1211–1227. doi: 10.1104/pp.104.054999
- Ramon, M., De Smet, I., Vandesteene, L., Naudts, M., Leyman, B., Van Dijck, P., et al. (2009). Extensive expression regulation and lack of heterologous enzymatic activity of the Class II trehalose metabolism proteins from *Arabidopsis thaliana*. *Plant Cell Environ.* 32, 1015–1032. doi: 10.1111/j.1365-3040.2009.01985.x
- Ronquist, F., and Huelsenbeck, J. P. (2003). MrBayes 3: Bayesian phylogenetic inference under mixed models. *Bioinformatics* 19, 1572–1574. doi: 10.1093/bioinformatics/btg180
- Rüegger, S., and Grosshans, H. (2012). MicroRNA turnover: when, how and why. *Trends Biochem. Sci.* 37, 436–446. doi: 10.1016/j.tibs.2012.07.002
- Schluepmann, H., and Paul, M. (2009). “Trehalose metabolites in Arabidopsis – elusive, active and central” in *The Arabidopsis Book*, eds R. Last, C. Chang, G. Jander, D. Kliebenstein, R. McClung, H. Millar, K. Torii, and D. Wagner (Washington, DC: American Society of Plant Biologists), 1–17.
- Schmutz, J., McClean, P. E., Mamidi, S., Wu, G. A., Cannon, S. B., Grimwood, J., et al. (2014). A reference genome for common bean and genome-wide analysis of dual domestications. *Nat. Genet.* 46, 707–713. doi: 10.1038/ng.3008
- Searle, I. R., Men, A. E., Laniya, T. S., Buzas, D. M., Iturbe-Ormaetxe, I., Carroll, B. J., et al. (2003). Long-distance signaling in nodulation directed by a CLAVATA-like receptor kinase. *Science* 299, 109–112. doi: 10.1126/science.1077937
- Streeter, J. G. (1988). Inhibition of legume nodule formation and N₂-fixation by nitrate. *CRC Crit. Rev. Plant Sci.* 7, 1–23. doi: 10.1080/07352688809382257
- Suárez, R., Wong, A., Ramírez, M., Barraza, A., Orozco Md, C., Cevallos, M. A., et al. (2008). Improvement of drought tolerance and grain yield in common bean by overexpressing trehalose-6-phosphate synthase in Rhizobia. *Mol. Plant-Microbe Interact.* 21, 958–966. doi: 10.1094/MPMI-21-7-0958
- Sugawara, M., Cytryn, E. J., and Sadowsky, M. J. (2010). Functional role of *Bradyrhizobium japonicum* trehalose biosynthesis and metabolism genes during physiological stress and nodulation. *Appl. Environ. Microbiol.* 76, 1071–1081. doi: 10.1128/AEM.02483-09
- Thibivilliers, S., Joshi, T., Campbell, K. B., Scheffler, B., Xu, D., Cooper, B., et al. (2009). Generation of *Phaseolus vulgaris* ESTs and investigation of their regulation upon *Uromyces appendiculatus* infection. *BMC Plant Biol.* 9:46. doi: 10.1186/1471-2229-9-46
- Thompson, J. D., Gibson, T. J., Plewniak, F., Jeanmougin, F., and Higgins, D. G. (1997). The CLUSTAL_X windows interface: flexible strategies for multiple

- sequence alignment aided by quality analysis tools. *Nucleic Acids Res.* 25, 4876–4882. doi: 10.1093/nar/25.24.4876
- Trainer, M. A., Capstick, D., Zachertowska, A., Lam, K. N., Clark, S. R., and Charles, T. C. (2010). Identification and characterization of the intracellular poly-3-hydroxybutyrate depolymerase enzyme PhaZ of *Sinorhizobium meliloti*. *BMC Microbiol.* 10:92. doi: 10.1186/1471-2180-10-92
- Valdés-López, O., Arenas-Huetero, C., Ramírez, M., Girard, L., Sánchez, F., Vance, C. P., et al. (2008). Essential role of MYB transcription factor: PvPHR1 and microRNA: PvmiR399 in phosphorus-deficiency signalling in common bean roots. *Plant Cell Environ.* 31, 1834–1843. doi: 10.1111/j.1365-3040.2008.01883.x
- Vandesteene, L., López-Galvis, L., Vanneste, K., Feil, R., Maere, S., Lammens, W., et al. (2012). Expansive evolution of the trehalose-6-phosphate phosphatase gene family in Arabidopsis. *Plant Physiol.* 160, 884–896. doi: 10.1104/pp.112.201400
- Van Houtte, H., Vandesteene, L., López-Galvis, L., Lemmens, L., Kissel, E., Carpentier, S., et al. (2013). Overexpression of the trehalase gene AtTRE1 leads to increased drought stress tolerance in Arabidopsis and is involved in abscisic acid-induced stomatal closure. *Plant Physiol.* 161, 1158–1171. doi: 10.1104/pp.112.211391
- Varkonyi-Gasic, E., Lough, R. H., Moss, S. M., Wu, R., and Hellens, R. P. (2012). Kiwifruit floral gene APETALA2 is alternatively spliced and accumulates in aberrant indeterminate flowers in the absence of miR172. *Plant Mol. Biol.* 78, 417–429. doi: 10.1007/s11103-012-9877-2
- Vauclare, P., Bligny, R., Gout, E., De Meuron, V., and Widmer, F. (2010). Metabolic and structural rearrangement during dark-induced autophagy in soybean (*Glycine max* L.) nodules: an electron microscopy and 31P and 13C nuclear magnetic resonance study. *Planta* 231, 1495–1504. doi: 10.1007/s00425-010-1148-3
- Vessey, J. K. (1994). Measurement of nitrogenase activity in legume root nodules: in defence of the acetylene reduction assay. *Plant Soil* 158, 151–162. doi: 10.1007/BF00009490
- Vlasova, A., Capella-Gutiérrez, S., Rendón-Anaya, M., Hernández-Oñate, M., Minoche, A. E., Erb, I., et al. (2016). Genome and transcriptome analysis of the Mesoamerican common bean and the role of gene duplications in establishing tissue and temporal specialization of genes. *Genome Biol.* 17, 32. doi: 10.1186/s13059-016-0883-6
- Vogel, G., Aeschbacher, R. A., Müller, J., Boller, T., and Wiemken, A. (1998). Trehalose-6-phosphate phosphatases from *Arabidopsis thaliana*: identification by functional complementation of the yeast tps2 mutant. *Plant J.* 13, 673–683. doi: 10.1046/j.1365-3113X.1998.00064.x
- Vogel, G., Fiehn, O., Jean-Richard-dit-Bressel, L., Boller, T., Wiemken, A., Aeschbacher, R. A., et al. (2001). Trehalose metabolism in Arabidopsis: occurrence of trehalose and molecular cloning and characterization of trehalose-6-phosphate synthase homologues. *J. Exp. Bot.* 52, 1817–1826.
- Voinnet, O. (2009). Origin, biogenesis, and activity of plant microRNAs. *Cell* 136, 669–687. doi: 10.1016/j.cell.2009.01.046
- Wahl, V., Ponnu, J., Schlereth, A., Arrivault, S., Langenecker, T., Franke, A., et al. (2013). Regulation of flowering by trehalose-6-phosphate signaling in *Arabidopsis thaliana*. *Science* 339, 704–707. doi: 10.1126/science.1230406
- Wang, Y., Wang, L., Zou, Y., Chen, L., Cai, Z., Zhang, S., et al. (2014). Soybean miR172c targets the repressive AP2 transcription factor NNC1 to activate ENOD40 expression and regulate nodule initiation. *Plant Cell* 26, 4782–4801. doi: 10.1105/tpc.114.131607
- Wilson, R. A., Gibson, R. P., Quispe, C. F., Littlechild, J. A., and Talbot, N. J. (2010). An NADPH-dependent genetic switch regulates plant infection by the rice blast fungus. *Proc. Natl. Acad. Sci. U.S.A.* 107, 21902–21907. doi: 10.1073/pnas.1006839107
- Wilson, R. A., Jenkinson, J. M., Gibson, R. P., Littlechild, J. A., Wang, Z. Y., and Talbot, N. J. (2007). Tps1 regulates the pentose phosphate pathway, nitrogen metabolism and fungal virulence. *EMBO J.* 26, 3673–3685. doi: 10.1038/sj.emboj.7601795
- Wingler, A., Delatte, T. L., O'Hara, L. E., Primavesi, L. F., Jhurrea, D., Paul, M. J., et al. (2012). Trehalose 6-phosphate is required for the onset of leaf senescence associated with high carbon availability. *Plant Physiol.* 158, 1241–1251. doi: 10.1104/pp.111.191908
- Wollmann, H., Mica, E., Todesco, M., Long, J. A., and Weigel, D. (2010). On reconciling the interactions between APETALA2, miR172 and AGAMOUS with the ABC model of flower development. *Development* 137, 3633–3642. doi: 10.1242/dev.036673
- Zhu, Q. H., and Helliwell, C. A. (2011). Regulation of flowering time and floral patterning by miR172. *J. Exp. Bot.* 62, 487–495. doi: 10.1093/jxb/erq295

Conflict of Interest Statement: The authors declare that the research was conducted in the absence of any commercial or financial relationships that could be construed as a potential conflict of interest.

Copyright © 2016 Barraza, Contreras-Cubas, Estrada-Navarrete, Reyes, Juárez-Verdayes, Avonce, Quinto, Díaz-Camino and Sanchez. This is an open-access article distributed under the terms of the Creative Commons Attribution License (CC BY). The use, distribution or reproduction in other forums is permitted, provided the original author(s) or licensor are credited and that the original publication in this journal is cited, in accordance with accepted academic practice. No use, distribution or reproduction is permitted which does not comply with these terms.